Journal of Non-Oxide Glasses Vol. 11, No. 4, October - December 2019, p. 65 - 71

STUDY OF IRON (III) SENSOR BASED ON CHALCOGENIDE GLASS

M. ESSI [a,*], D. COT [b]
[a]*Laboratoire de Chimie des Matériaux Inorganiques, Université Félix HOUPHOUET-BOIGNY de Cocody, UFR-SSMT, 22 BP 582 Abidjan 22, Côte d'Ivoire.*
[b]*Institut Européen des Membranes, Université de Montpellier, 34095 Montpellier cedex 5, France*

This paper presents a preliminary structural and electrochemical study of the iron chalcogenide glass Fe-selective electrode using X-ray diff raction (XRD) and scanning electron microscopy (SEM). The electrochemical characterization of a chalcogenide-based iron membrane was achieved by means of a direct potentiometric measurement. We used differential scanning calorimetry (DSC) analysis to check the calorimetric evolution of the as-quenched specimens under a continuous heating. Sensor response versus Fe^{3+} has been examined, and a response mechanism is proposed. Studied sensor exhibits a slope of 30 mV/decade in a large range of primary ion concentration. The electrode has a short response time and has a good selectivity towards a lot of foreign species. The sensor was used for a period of one month without significant shift of potential electrode. The results of this study have provided a response mechanism involving a combination of charge transfer and ion-exchange of Fe^{3+} species.

(Received August 4, 2019; Accepted November 20, 2019)

Keywords: Chalcogenide glass, In situ monitoring, Heavy metal ion, Iron-selective Electrode, Iron

1. Introduction

Iron is an important limiting trace metal nutrient in marine waters [1-4], as it limits the growth of phytoplankton and biomass production in the ocean. Recent work has demonstrated that iron limitation is important in regions characterised by high nutrients and low chlorophyll such as the eastern equatorial Pacific, the Pacific subarctic and the Southern Ocean [5] in agreement with previous work [4, 5]. While there is an array of ex situ techniques that can be employed in the determination of iron (III) in seawater [6] these methods are susceptible to experimental uncertainties [7-9]. It has been established that ion-selective electrodes offer an alternative method for the electroanalysis of metal species in environmental samples since they are suitable for metal ion in situ monitoring [6, 10-14]. The development of chalcogenide-based potentiometric chemical sensors may not be surprising considering that chalcogenide glasses are chemically more stable in a wide range of media compared to their crystalline counterparts [15-19]. Moreover, the fact that bulk glasses are easily obtained makes chalcogenide matrix an ideal system to investigate a great variety of properties and their correlation with structure and composition [20-22]. Chalcogenide glasses are materials that comprise any one of the chalcogen elements which are located in group 6 of the periodic table. Chalcogenide glass-based ISEs have been introduced by Baker and Trachtenberg in the 1970s [23, 24]. A systematic progress with chalcogenide glass materials in of investigating the sensing mechanism has been made [25-29]. One of the widely used Fe (III) selective electrodes is based on a chalcogenide system Fe_x $[Ge_{28}Sb_{12}Se_{60}]_{100-x}$. Early work by Vlasov, Bychkov and Legin demonstrated satisfying out put signal with the Fe(III)-SE [28, 30]. Further studies confirmed that Fe ISE can be calibrated in continuous flow analysis with a great detection limit [4]. On the other hand, potentiometric sensor based on inorganic membrane can be used for Fe^{3+} ions detection [31]. Despite the consensus on the electron transfer mechanism for

* Corresponding author: marc.essi@netcourrier.com

Fe^{3+} response of the iron chalcogenide glass electrode, there are several inconsistencies related to the slopes of Fe-ISE response curves. Studying the physical properties and electrochemical characteristics our goal was to understand the ISE response versus iron species. $Fe_x[Ge_{28}Sb_{12}Se_{60}]_{100-x}$ sensor was tested under stationary conditions in waste waters.

2. Experimental

We selected the $Ge_{28}Sb_{12}Se_{60}$ glassy matrix as a base matrix, since the $Ge_{28}Sb_{12}Se_{60}$ material is well known homogeneous bulk glasses, commercialized by Vitron under the reference IG5® [32], which indicates the commercial importance of the materials under study. The Fe (III) ISE is based on a bulk chalcogenide glass of composition $Ge_{28}Sb_{12}Se_{60}$ which is a wide-gap electronic insulator, and the addition of iron [i.e., Fe_x $(Ge_{28}Sb_{12}Se_{60})_{100-x}$] has been shown to greatly enhance membrane conductivity. Therefore the iron (III) selective electrode is based on the following composition, $Fe_{2.5}$ $[Ge_{28}Sb_{12}Se_{60}]_{97.5}$ which has been recently applied for the determination of the Fe^{3+} species in marine water [4].

For preparing the sensing devices, selenium powder (99.5%), germanium metal (99.9999%), antimony metal (99.999%) obtained from Aldrich Chemical Co. and iron powder (96% due to aerial oxidation of the fine particulates) from Ajax Chemical Co. Pty. Ltd. were mixed in the appropriated proportions. Stoichiometric proportions of the reactants were loaded into 10 mm diameter quartz tubes. A total weight of 3 g was used, and the evacuated ampoule was sealed prior to heating. The loaded tubes were evacuated to 10^{-5} mbar and sealed. The ampoule was heated for 24 h at 1030 °C. The tubes containing the melt were continuously rotated to ensure complete mixing and reaction. Melts were rapidly quenched by immersing the ampoules into an ice–water bath. The resultant melt was air quenched, and annealed for 2 h at 200±10 °C to remove excess stress within the glass.

Structural characteristics of the materials were checked by X-ray diffraction. The XRD measurements were performed using a SEIFERT diffractometer with Cu Kα radiation (λ = 1.5406 Å). An operating voltage of 40 kV and a beam current of 25 mA were selected.

The elemental composition and surface topography of the sensor were performed using energy-dispersive X-ray spectrometry (EDS), interfaced to the scanning electron microscopy.

To prepare sensors, disc having few mm in thickness and a diameter of ten mm were cut from the ingot. In order to undertake meaningful surface and electrochemical studies of the Fe (III) chalcogenide ISE, it was necessary to clean the membrane surface prior to analysis. This was accomplished by using Struers silicon carbide paper of various grit size. The membranes were subsequently polished extensively in a methodical stepwise approach by utilizing diamond spray of decreasing sizes. The electrode was washed with Milli-Q water and blotted dry on tissue before use. A metallic layer was sputtered on one side and a wire was attached with a silver micro adhesive. Then the inner side was coated with and epoxy resin to produce a sensing device.

Table 1. Cation concentrations of waste solution measured by Inductive Coupled Plasma.

Species	**Tl**	**Cr**	**Mn**	**Co**	**Ni**	**Cu**	**Zn**	**As**	**Sr**	**Cd**	**Sb**	**Ba**	**Tl**	**Mg**
activity ($\mu g.L^{-1}$)	22105	33	7309	264	486	277	16930	153930	200	69	42	19	294	1339

The electrode potential was measured with a high impedance millivoltmeter. The change of the potential, depending of the concentration of the analyte, can be measured against a conventional reference electrode by means of a direct potentiometric measurement. The external reference electrode was a saturated Ag/AgCl electrode used with a double junction. Concentrations were used instead of activities because all measurements were carried out in solutions with constant ionic strength prepared with 10^{-1} M KNO_3 as a background electrolyte. Calibrations were performed in the concentration range 10^{-7} – 10^{-3} M by addition of known volume of iron (II) test

solutions to 100 ml of electrolyte solution. Calibrations were performed under stationary conditions (i.e. analyte change by hand and electrolyte movement by means of magnet agitators during the potential measurement). Test solutions in the concentration range 10^{-1} – 10^{-4} M were prepared by successive ilutions of a 1M Fe^{3+} solution by the KNO_3 (10^{-1} M) supporting electrolyte. The measurement time between each concentration step was 4 min. **Table 1** presents cation concentrations measured by ICP-AES of Waste waters. Polluted waters were filtered and kept at low temperature.

3. Results

We used DSC analysis to check the calorimetric evolution of the as-quenched specimens under a continuous heating. All powder samples weighting 10 mg were sealed in aluminium pans. Continuous heating experiments were performed at scan rates 10 °C.min^{-1}. The measurement temperatures were attained heating the amorphous samples from room temperature to 500°C. The calorimetric curves show a shift of the base line consequent with the heat capacity changes from the glass to the undercooled liquid state at the glass transition. Glass transition temperature was found to reach a low value (i. e. below 200° C) at elevated iron dopant (i. e. 2.0 to 2.5 at. %). X-ray analysis was used for the determination of the vitreous state. Microscopy and EDX were used to check material uniformity and homogeneity.

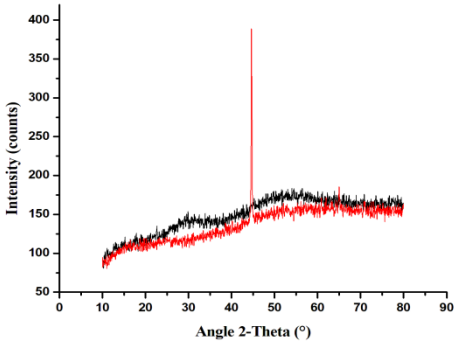

Fig. 1. Powder XRD patterns of bulk membrane (black) and Fe starting material (red).

Fig. 1 illustrates the X-ray difraction (XRD) patterns of bulk sensing membrane and starting material. These patterns are characterized by the presence of a centered hump indicating an amorphous state of the sensitive material. Moreover, we confirmed the crystalline state of high purity starting material. X-ray data are in agreement with previous studies. It has been shown that the glass is mostly amorphous. However, the presence of some crystallinity has been witnessed at elevated iron contents. Some reports suggest that the chalcogenide membrane comprises clusters of a second phase dispersed in the glass matrix at elevated iron dopant levels (i. e. >2.0 at. %), and this has a profound influence on the bulk electrical conductivity of the membrane [23]. In our case, due to poor crystallinity we did not identified secondary crystalline phase. Then, further X-ray analysis are in progress in order to elucidate optimum experimental parameters.

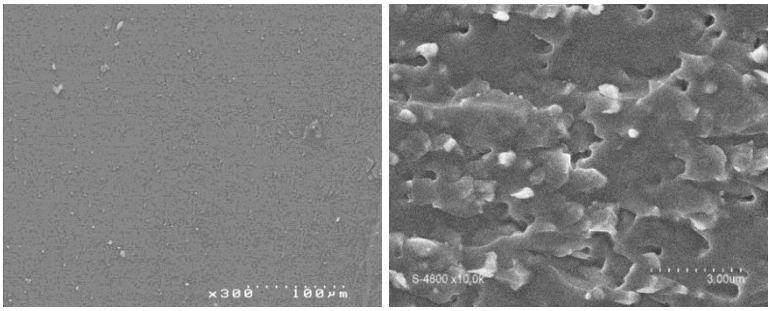

(a) *(b)*

Fig. 2. SEM micrographs of the studied Fe-SE (a) and Cu_{10} $(As_2S_3)_{90}$ sensor (b).

As shown in Fig. 2, SEM observations indicated a heterogeneous multiphase system with a crystalline material embedded in an amorphous chalcogenide matrix. Similar results are observed for Cu_x-$(As_2S_3)_{1-x}$. As reported elsewhere [33], SEM observations and X-ray diffraction indicate that the Cu_{10}–$(As_2S_3)_{90}$ alloy consists in crystallites of sinnerite embedded in an amorphous matrix. Further EPMA analysis is needed to elucidate crystalline phase composition in our samples. An extensive step-by-step study of the sensing matrix chemical composition has been done. EDX was used for this study. The composition topography of the surface has been investigated along the length of the chalcogenide sample. Due to a contamination, C is detected. It is demonstrated that the composition was constant throughout the depth of the bulk device. Figure 3 indicated a homogeneous distribution of elements. EDX data (Table 2) demonstrated that the relative amount of all elements was closed to the theoretical composition of the glassy matrix. On the whole the data obtained by EDX indicated that bulk membrane was homogeneous in composition and was poorly contaminated. The sensitive membrane has a surface of good quality.

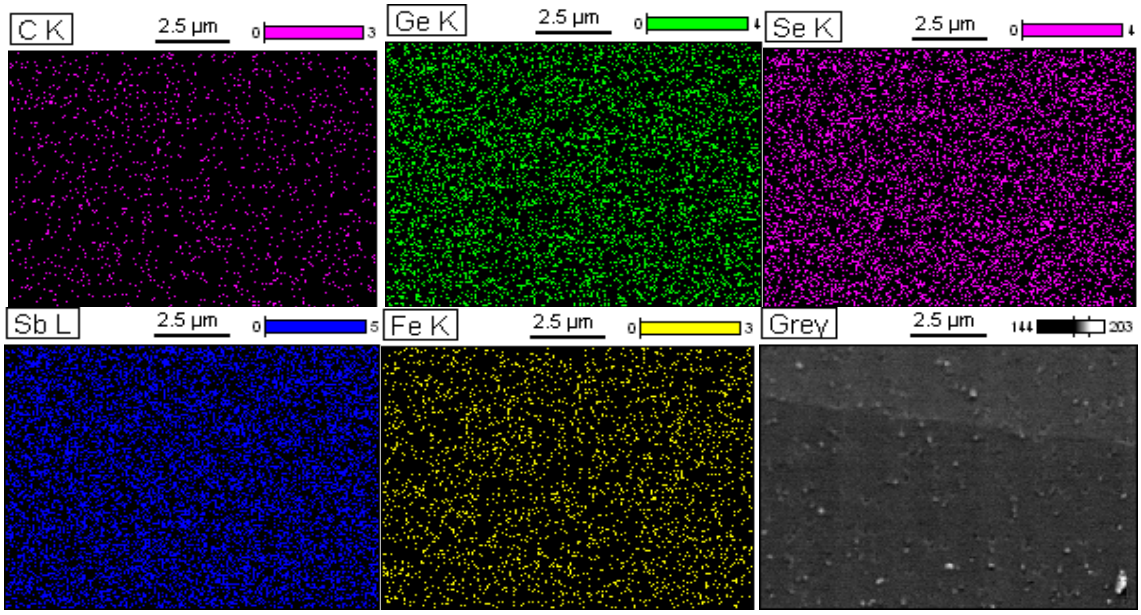

Fig. 3. The composition topography of the studied sensor by EDX and SEM micrograph of the analysed surface (grey).

Table 2. Chemical composition of the bulk sensing membrane measured by EDX.

Elemental concentration (at.%)					Sample
C	**Fe**	**Ge**	**Sb**	**Se**	
39,79	1,98	16,43	8,22	33,58	Fresh Sample
	x	28(1-x)	12(1-x)	60(1-x)	Theoretical Sample

The response of bulk sensor to iron (III) ions was checked. Prior to out-put signal measurements, all the sensors were conditioned for 17 h by soaking in 10^{-5} M $FeCl_3.6H_20$ solution. The best results were obtained for the membrane in a linear range from 3.10^{-5} – 10^{-2} M with a slope of 30 mV/decade. We demonstrated that the detection limit of the Fe (III) ISE in iron (III) solutions is 10^{-6} M. The detection limit was established at the point of intersection of the extrapolated linear mid-range and final low concentration level segments of the calibration plot (Fig. 4). The measuring principle of the ion-selective electrode method is well established. The Fe-ISE contains sensing bulk material composed of active layers, which has high selectivity to Fe^{3+} species in solution, thus produces a certain electromotive force. The ion concentration can be calculated by the electromotive force which is generated between Fe-SE and reference electrode. The sensor potentiometric response obeyed the Nernst law:

$$EMF = K + \frac{RT}{zF}\log\left[Fe^{3+}\right]$$

where, EMF is the electromotive force (the observed potential at zero current). K is a constant potential contribution that often includes the liquid-junction potential at the reference electrode. $[Fe^{3+}]$ is the sample activity for the ion Fe^{3+} with charge z and R, T and F are the gas constant, absolute temperature and Faraday constant respectively.

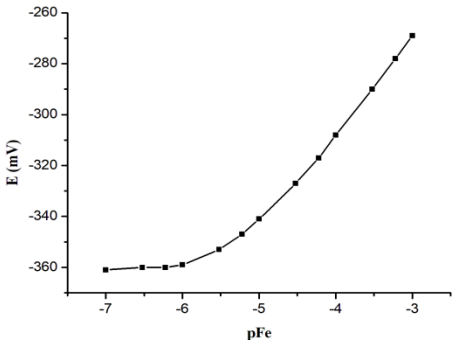

Fig. 4. Potentiometric response of studied bulk sensor.

Previous work reported that an optimum doping level of 2.0 at.% iron is required for near Nernstian response, potential stability and response time characteristics [23, 24]. The stability and reproducibility of the Fe (III)-sensor were also tested. The standard deviation of several replicate measurements made for high level of primary ion concentration was ± 2 mV. The sensor was used for a period of one month without significant changes of response versus Fe (III) ion. The experimental response time of the sensor to reach 95% of the equilibrium potential was about 10 s as the concentration of iron (III) varies from 10^{-4} to 10^{-3} M. The electrode showed high selectivity with respect to alkaline and heavy metal ions. To determine the selectivity coefficients we used the fixed interference method. The out-put signal was recorded with solutions of constant level of interference and a varying concentration of the Fe^{3+} ion. The sensitivity of the electrode was investigated in the presence various species. As it could be expected, the sensor has very good

values of the selectivity coefficients, especially toward Co^{2+}, Ni^{2+} and Li^{+}. Common interfering ionic species such as copper, lead, nickel do not interfere with the iron response. The selectivity data are comparable to those already reported for similar bulk and thin film chalcogenide ISE [14]. The response characteristics of the studied iron sensor have been established in well-defined electrolytes. However, the ISE response mechanism is not well understood and has been the subject of some recent controversy. There are several inconsistencies related to the slopes of Fe (III)-SE calibration curves with most studies reporting of 30-50 mv/decade change in the activity of Fe^{3+} species in unbuffered solution which is much lower than the Nernstian prediction of 59.16 mv/decade for one electron charge transfer process. Previous work undertook a detailed study of the response mechanism of the iron (III) sensing electrode in saline media. The observed slope of 30 mv/decade was inconsistent with the expected value for trivalent ion-exchange of Fe(III) (i.e., 19.72 mv/decade) or the one predicted for a one electron transfert process (i.e., 59.16 mv/decade). Instead, authors inferred theoretically a mixed reaction mechanism involving both electron transfer and ion-exchange processes. A mechanism involving a combination of charge transfer and ion-exchange of Fe^{3+} species, at the membrane/solution interface, can be used to explain the 30 mV/decade slope of the selective electrode. Particularly, the charge transfer sensitivity of this sensor necessitates the presence of the Fe(II)/Fe(III) redox couple in the modified surface layer of the electrode. While the Fe^{3+} ion exchange mechanism requires a presence of Fe^{3+} primary ion in the modified surface layer that behaves like an Fe (III) ion exchanger or selective Fe (III) conducting electrolyte. Most workers agree that the mechanism is probably electronic rather than ionic [23, 24]. It is of interest to note that the mechanism of Cu_x $(Ge_{28}Sb_{12}Se_{60})_{100-x}$ Nerstian response to Cu^{2+} is different [8].

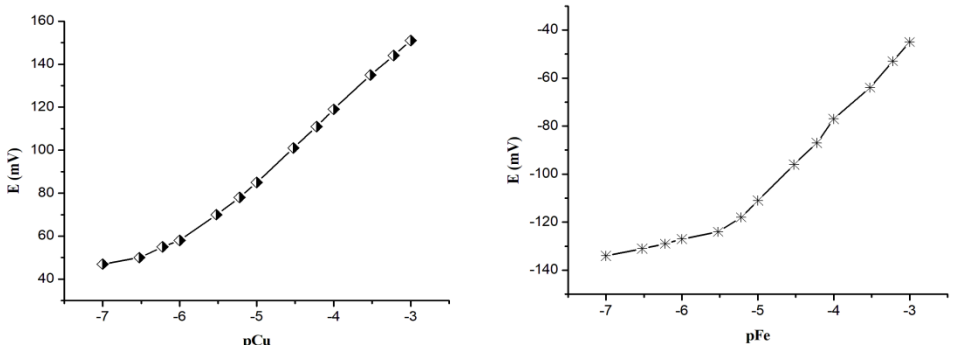

Fig. 5. Cu_x $[Ge_{28}Sb_{12}Se_{60}]_{1-x}$ thin membrane response versus Cu^{2+} (a) and Fe_x $[Ge_{28}Sb_{12}Se_{60}]_{100-x}$ bulk membrane response versus Fe^{3+} (b) in polluted sample (Table 1).

The final aim of the work was to provide in situ analysis in waste waters. Then, measurements have been carried out in polluted solutions. In agreement with electrochemical study measurements have shown a good reproducibility and long term stability. On the whole the data obtained in Fig. 5 indicated that the sensors allow simultaneous detection of Cu^{2+} and Fe^{3+} species in waste waters.

4. Conclusions

SEM observations indicated a heterogeneous multiphase system with a crystalline material embedded in an amorphous chalcogenide matrix. EDX indicated that bulk membrane was homogeneous in composition and was poorly contaminated with a surface of good quality. The best results were obtained for the membrane in a linear range from 3.10^{-5} – 10^{-2} M with a slope of 30 mV/decade. We demonstrated that the detection limit of the Fe (III) ISE in iron (III) solutions is 10^{-6} M. The sensor was used for a period of one month without significant changes of response

versus Fe (III) ion. The average response time of the sensor was about 10 s. The electrode showed high selectivity with respect to alkaline, heavy metal ions and common interfering ionic species such as copper, lead, nickel. A mechanism involving a combination of charge transfer and ion-exchange of Fe^{3+} species, at the membrane/solution interface, can be used to explain the 30 mV/decade slope of the selective electrode. This study demonstrated that potentiometric response characteristics of Fe-ISE allow reliable measurements of Fe^{3+} species in solution. Studied chalcogenide based devices allow simultaneous in situ monitoring of Cu^{2+} and Fe^{3+} species in waste waters.

References

[1] M. Gledhill, C. M. G. van den Berg. Mar. Chem. **47**, 41 (1994).
[2] E. L. Rue, K. W. Bruland. Mar. Chem. **50**, 117 (1995).
[3] F. J. Millero, W. Yao, J. Aicher. Mar. Chem. **50**, 21 (1995).
[4] R. De Marco, J. Martizano. Talanta **75**, 1234 (2008).
[5] R. De Marco, D.J. Mackey. Mar. Chem. **68**, 283 (2000).
[6] B. Pejcic et al. Talanta **63**, 149 (2004).
[7] F. O. Méar, M. Essi, P. Sistat, P. Huguet, A. Pradel, M. Ribes, in: Proceedings of the 21st International Conference on Solid Waste Technology and Management (ICSWM), Philadelphia, PA (USA), 2006.
[8] F. O. Méar, M. Essi, P. Sistat, M.-F. Guimon, D. Gonbeau, A. Pradel, Appl. Surf. Sci. **255**, 6607 (2009).
[9] F. O. Méar, M. Essi, M.-F. Guimon, A. Pradel, Chalcogen. Lett. **5**, 117 (2008).
[10] B. Pejcic, R. De Marco, Electrochim. Acta **49**, 3525 (2004).
[11] Xin Wang et al. Procedia Eng. **15**, 2609 (2011).
[12] M. Essi, Chalcogen. Lett. **8**, 301 (2011).
[13] M. Essi, Chalcogen. Lett. **8**, 25 (2011).
[14] M. Essi, A. Pradel, Chalcogen. Lett. **8**, 15 (2011).
[15] V. S. Vassilev, S. V. Boycheva, Talanta **67**, 20 (2005).
[16] M. Essi, Chalcogen. Lett. **8**, 341 (2011).
[17] M. Essi, Journal of Non-Oxide Glasses **3**, 8 (2011).
[18] M. Essi, Chalcogen. Lett. **8**, 103 (2011).
[19] M. ESSI, J. Non-Oxide Glasses **3**, 67 (2011).
[20] M. A. Urena et al., J. Non-Cryst. Solids **320**, 151 (2003).
[21] A. M. Salem et al., Nucl. Instr. and Meth. in Phys. Res. B **262**, 225 (2007).
[22] M. ESSI, P. Yot, G. Chevallier, C. Estournes, A. Pradel, Dig. J. Nanomater. Bios. **6**, 1777 (2011).
[23] C. T. Baker, I. Trachtenberg, J. Electrochem. Soc. **118**, 571 (1971).
[24] R. Jasinski, I. Trachtenberg, J. Electrochem. Soc. **120**, 1169 (1973).
[25] M. Essi, B. Kedi, Chalcogen. Lett. **16**, 29 (2019).
[26] M. Essi, N. Kouame, G. Cisse. Chalcogen. Lett. **15**, 379 (2018).
[27] M. Maric et al., Electrochem. Commun. **41**, 27 (2014).
[28] Yu. G. Vlasov et al., Talanta **41**, 1059 (1994).
[29] M. J. Schoning, J. P. Kloock, Electroanalysis **19**(2), 007 (2019).
[30] Yu. G. Vlasov, E. A. Bychkov J. Electroanal. Chem. **378**, 201 (1994).
[31] D. Vlascici et al., Sensors **12**, 8193 (2012).
[32] V. Balan et al., J. Non-Cryst. Solids **326-327**, 455 (2003).
[33] C. Cali, D. Foix, G. Taillades, E. Siebert, D. Gonbeau, A. Pradel, M. Ribes, Mater. Sci. Eng. C **21**, 3 (2002).